Transmission Benefits of Co-Locating Concentrating Solar Power and Wind

Ramteen Sioshansi
The Ohio State University

Paul Denholm
National Renewable Energy Laboratory

Transmission Benefits of Co-Locating Concentrating Solar Power and Wind

Ramteen Sioshansi
The Ohio State University

Paul Denholm
National Renewable Energy Laboratory

National Renewable Energy Laboratory
1617 Cole Boulevard
Golden, Colorado 80401
303-275-3000 • www.nrel.gov

NOTICE

This report was prepared as an account of work sponsored by an agency of the United States government. Neither the United States government nor any agency thereof, nor any of their employees, makes any warranty, express or implied, or assumes any legal liability or responsibility for the accuracy, completeness, or usefulness of any information, apparatus, product, or process disclosed, or represents that its use would not infringe privately owned rights. Reference herein to any specific commercial product, process, or service by trade name, trademark, manufacturer, or otherwise does not necessarily constitute or imply its endorsement, recommendation, or favoring by the United States government or any agency thereof. The views and opinions of authors expressed herein do not necessarily state or reflect those of the United States government or any agency thereof.

Available electronically at http://www.osti.gov/bridge

Available for a processing fee to U.S. Department of Energy
and its contractors, in paper, from:

> U.S. Department of Energy
> Office of Scientific and Technical Information
> P.O. Box 62
> Oak Ridge, TN 37831-0062
> phone: 865.576.8401
> fax: 865.576.5728
> email: mailto:reports@adonis.osti.gov

Available for sale to the public, in paper, from:

> U.S. Department of Commerce
> National Technical Information Service
> 5285 Port Royal Road
> Springfield, VA 22161
> phone: 800.553.6847
> fax: 703.605.6900
> email: orders@ntis.fedworld.gov
> online ordering: http://www.ntis.gov/help/ordermethods.aspx

Cover Photos: (left to right) PIX 16416, PIX 17423, PIX 16560, PIX 17613, PIX 17436, PIX 17721

Printed on paper containing at least 50% wastepaper, including 10% post consumer waste.

Acknowledgment

List of Acronyms

CSP	concentrating solar power
DNI	direct normal irradiance
DOE	U.S. Department of Energy
EIA	Energy Information Administration
ERCOT	Electric Reliability Council of Texas
FERC	Federal Energy Regulatory Commission
GE	General Electric Corporation
GW	gigawatt
HTF	heat transfer fluid
ITC	investment tax credit
kW	kilowatt
kWh	kilowatt-hour
MIP	mixed-integer program
MW	megawatt
MW-e	megawatts electric capacity
MW-t	megawatts thermal capacity
MWh-e	megawatt-hours of electric energy
MWh-t	megawatt-hours of thermal energy
NERC	North American Electric Reliability Corporation
NREL	National Renewable Energy Laboratory
SAM	Solar Advisor Model
SM	solar multiple
TES	thermal energy storage

Executive Summary

This report discusses and analyzes the potential benefits of co-locating wind and concentrating solar power (CSP) plants in the southwestern United States. Using a location in western Texas as a case study, we demonstrate that such a deployment strategy can improve the capacity factor of the combined plant and the associated transmission investment. This is because of two synergies between wind and CSP. One is that real-time wind and solar resource availability tend to be slightly negatively correlated. The other is that low-cost and highly efficient thermal energy storage (TES) can be incorporated into CSP. TES allows solar generation to be shifted and used to fill-in excess transmission capacity not being used by wind. Adding TES in a transmission constrained system can reduce, but not eliminate curtailment, especially during periods of extended high wind output and high solar output. Adding transmission constraints associated with co-location also reduces performance, including the inability of CSP to provide maximum output during periods of both high demand and significant wind output. Overall the economic tradeoff between transmission costs and system performance is highly sensitive to assumptions regarding transmission and CSP costs. Using data from the years 2004 and 2005, we demonstrate that a number of deployment configurations, which include up to 56% CSP (on a capacity and energy basis) yield a positive net return on investment.

Table of Contents

List of Figures

List of Tables

1 Introduction

One of the challenges in deploying renewable electricity generation is the often remote location of high-quality wind and solar resources, requiring new transmission. The state of Texas was one of the first regions of the United States to contend with this issue. The highest quality wind resources are located in the western part of the state, while the major population centers are in the east. About 1.4 GW of wind was added in the McCamey region of Texas in 2001 and 2002, despite there only being about 400 MW-e of transmission capacity [1]. This resulted in about 380 GWh of wind generation being curtailed at an estimated cost of more than $21.4 million in 2002. Although substantial transmission capacity has been added, this construction has not kept pace with wind development, and nearly 8% of potential wind generation in the Electric Reliability Council of Texas (ERCOT) was curtailed in 2010 [2].

New transmission is often difficult to construct, and, if it is only carrying wind, these lines will tend to be lightly loaded due to the low capacity factor of the generator. For instance, a typical wind plant will have a capacity factor of less than 40%. One option to enhance utilization of new transmission is to co-locate wind with other resources that can complement their generation. This can include conventional generation, energy storage, or other renewables. Denholm and Sioshansi [3] demonstrate that energy storage is one viable option, since transmission can be downsized (relative to the capacity of the wind generator) and generation that would be curtailed can be stored for later use.

Another option is to deploy concentrating solar power (CSP) in areas with good wind resources. West Texas has good wind resources (at least class 4, which is defined as having average wind speeds of 7 m/s at a 50 m height) that are in close proximity to locations with sufficient direct normal irradiance (DNI) for economic siting of CSP plants (average daily DNI of at least 6 kWh/m^2 is typically viewed as the minimum solar resource requirement). CSP plants have an additional advantage of being able to incorporate low-cost and high-efficiency thermal energy storage (TES), enabling them to become a dispatchable resource.[1]

In this paper we examine the basic feasibility and performance of wind and CSP plants in western Texas that feed into the grid on a radial transmission line. We examine cases in which various combinations of wind and CSP are deployed with different amounts of transmission capacity. Using historical market price and weather data we model the operation of such a deployment and demonstrate how the dispatch, the capacity factor, energy curtailment, and the cost of energy are influenced by the combination of wind and CSP. The remainder of this paper is organized as follows: Section 2 provides further background on wind and CSP development, Section 3 discusses the methods and data used in the analysis, Section 4 summarizes our results, and Section 5 concludes.

---

[1] Although it is beyond the scope of this paper, there is a large literature detailing CSP and TES technologies, including performance and cost analyses [4-8].

2 Background

The Electric Reliability Council of Texas (ERCOT) is one of three North American interconnects, and had a peak system load of about 61 GW in 2005. The interconnects are electrically isolated alternating current networks. Although there are some tie lines between the interconnects, they largely operate in isolation of one another. The ERCOT region has sufficient wind and solar resources to meet the system's entire current electricity demand, however, its best wind and solar resources are in the western part of the state. This is illustrated in Figure 1, which overlays areas of Texas that have at least class-4 wind and a daily average DNI of at least 5 kWh/m^2. Figure 1 excludes areas that would be unsuitable for CSP and wind development, by filtering out environmentally sensitive lands, urban areas, water features, terrain with more than a 3% average land slope, and areas with less than 1 km^2 of contiguous land space. Figure 1 shows that not all of Texas is within the ERCOT system, however ERCOT accounts for about 85% of Texas's electricity demand. Figure 1 also shows the location studied in this analysis, which is discussed further in Section 3.
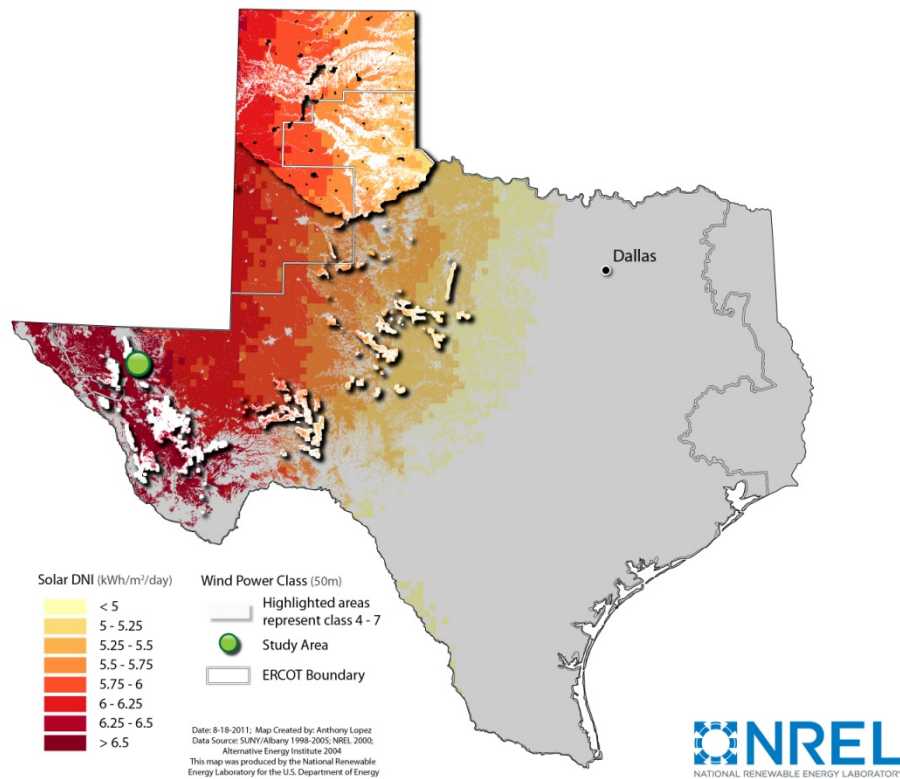
Figure 1. Average daily DNI of locations in Texas with at least class-4 wind.

At the end of 2010, ERCOT had installed 10 GW of wind, with the vast majority located in western Texas. Substantial transmission capacity has been added to access these resources and further transmission expansion is in the planning stages. However, the capacity of wind exceeds the transmission capacity, resulting in some wind curtailment. Given the variability of the wind

resource, and relatively low capacity factor, transmission built for wind will often be underutilized. This is illustrated in Figure 2, which is the average generation duration curve for the simulated wind plant in west Texas that we study in this analysis over the years 2004 and 2005. The modeled wind plant has a capacity factor of about 33.9%.
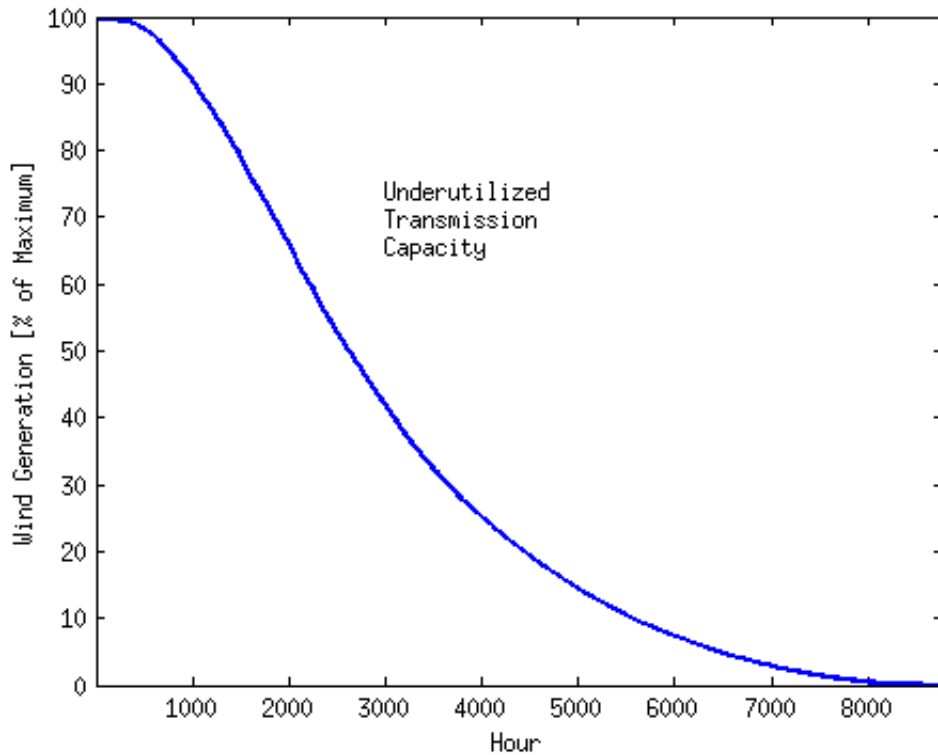
Figure 2. Average wind generation duration curve during the years 2004 and 2005 at the location modeled in this analysis.

CSP has yet to be developed in Texas, largely due to its substantially higher cost compared to wind. However the prospect of decreasing CSP costs [10], along with its ability to provide dispatchable energy, could result in CSP deployments in the future. CSP in ERCOT faces the same challenges as wind in requiring new transmission from western to eastern Texas. This increases the cost of a deployment and makes development more challenging. However, CSP has the opportunity to use transmission built primarily for wind. Due to the relatively low capacity factor of wind and the dispatchability of CSP with TES, CSP generation could "fill in" during periods of low wind output. This opportunity is represented by the large area above the wind duration curve where transmission capacity is available. Figure 3 illustrates two days of simulated wind data, beginning on January 9, 2005, on a transmission line sized at the peak output of the wind plant (the data are explained in more detail in Section 3). This shows the opportunity to dispatch CSP during periods of low wind output.
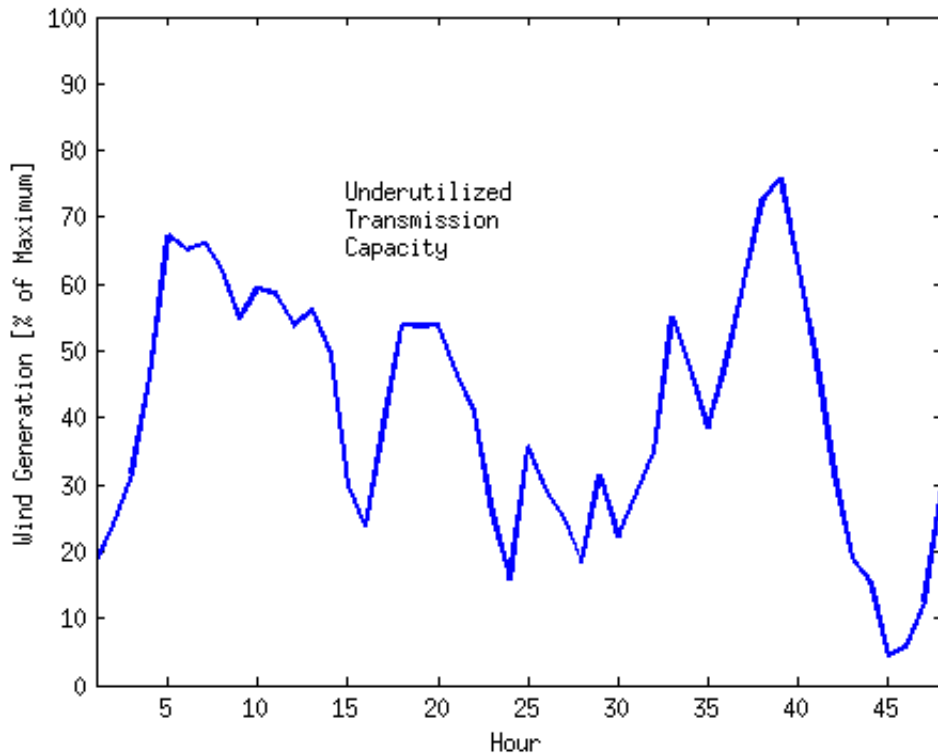
Figure 3. Example simulated wind output during a two-day period beginning on January 9, 2005 and opportunities to fill underutilized transmission capacity with other generation sources.

However, sharing transmission between resources does present several limitations. To maximize transmission utilization, the overall capacity of the transmission will be less than the combined maximum output of the CSP and wind plants. Ideally, CSP is dispatched to provide maximum output during periods of highest demand. Still, there may be periods during which CSP is forced to shift output to periods of lower demand (and correspondingly lower value) due to binding transmission constraints. In addition, there will likely be extended periods of time of both high wind and solar output, resulting in curtailed generation. Thus co-location of wind and CSP represents a tradeoff between maximizing the value of energy production and the cost of transmission development. The goal of this analysis is to examine this tradeoff and identify opportunities where it may be beneficial to co-locate wind and CSP and share transmission resources.

Although we examine a location in Texas, there are other locations in the southwestern United States that could support co-location of wind and CSP generation. Figure 4 illustrates this by overlaying areas of the southwestern United States that have at least class-4 wind with average daily DNI. This figure also filters out areas that are unsuitable for CSP and wind development. Thus this analysis could be applied to other potential sites where new, long-distance transmission is needed to access both wind and solar resources.
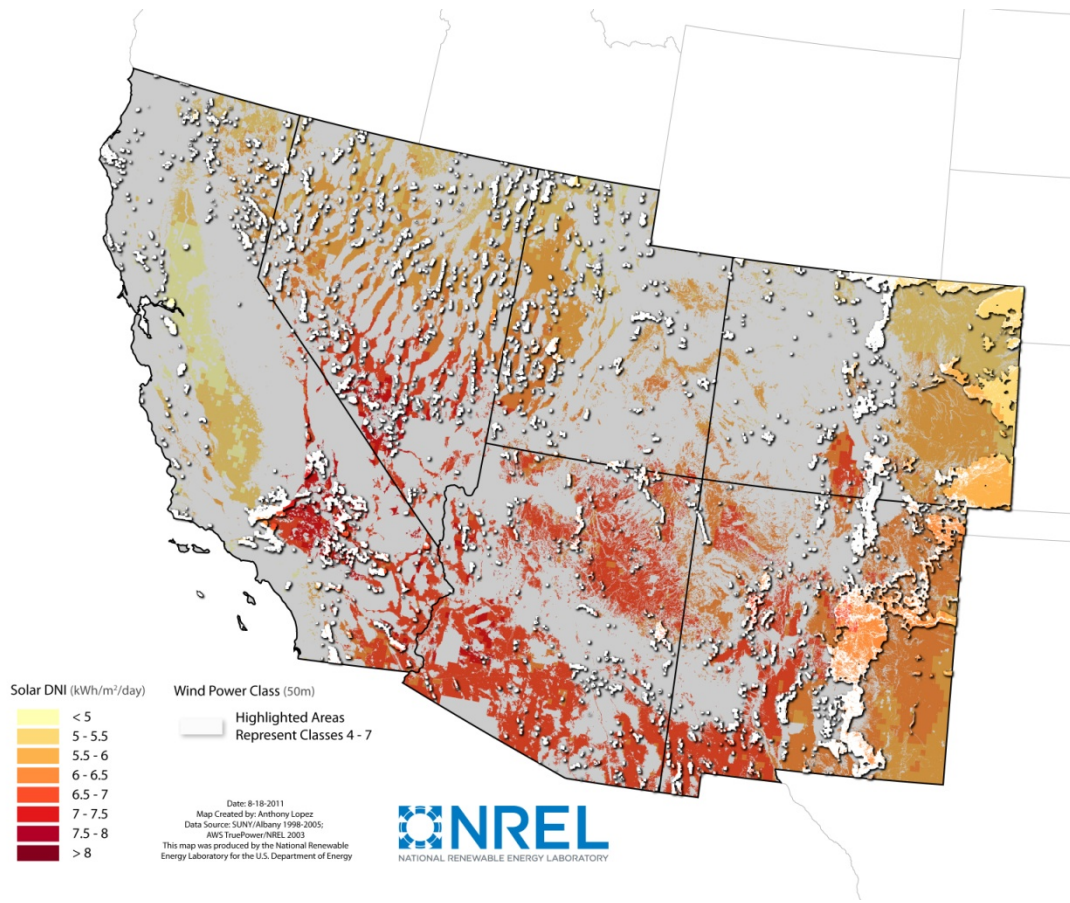
Figure 4. Average daily DNI of locations in the southwestern United States with at least class-4 wind.

3 Methods

We base our analysis on the CSP optimization model developed by Sioshansi and Denholm [9, 10]. The model takes the characteristics of the combined plant (e.g., number and size of CSP plants, installed wind capacity, transmission capacity), weather, and market price data as fixed, and optimizes the operation of the CSP and wind plants to maximize total revenues. We model CSP and wind plants at the location in western Texas that is shown in Figure 1. The details of this location are provided in Table 1 and Figure 5 shows a histogram of wholesale energy prices over the two-year period studied. The location is not optimized, but is a site with good wind and CSP resources. The site is located in a relatively unpopulated area, and would thus require major transmission investments to deliver energy to customers. We examine generator dispatch and resulting revenues during the years 2004 and 2005, for which high-resolution wind and solar resource data are available.

Table 1. Location Studied

Location:	31.49° N, 104.56° W
Interconnection Point:	Dallas
Linear Distance:	931 km
Market Pricing Location:	ERCOT North Zone
Transmission Distance:	1043 km
Transmission Losses:	4.9%
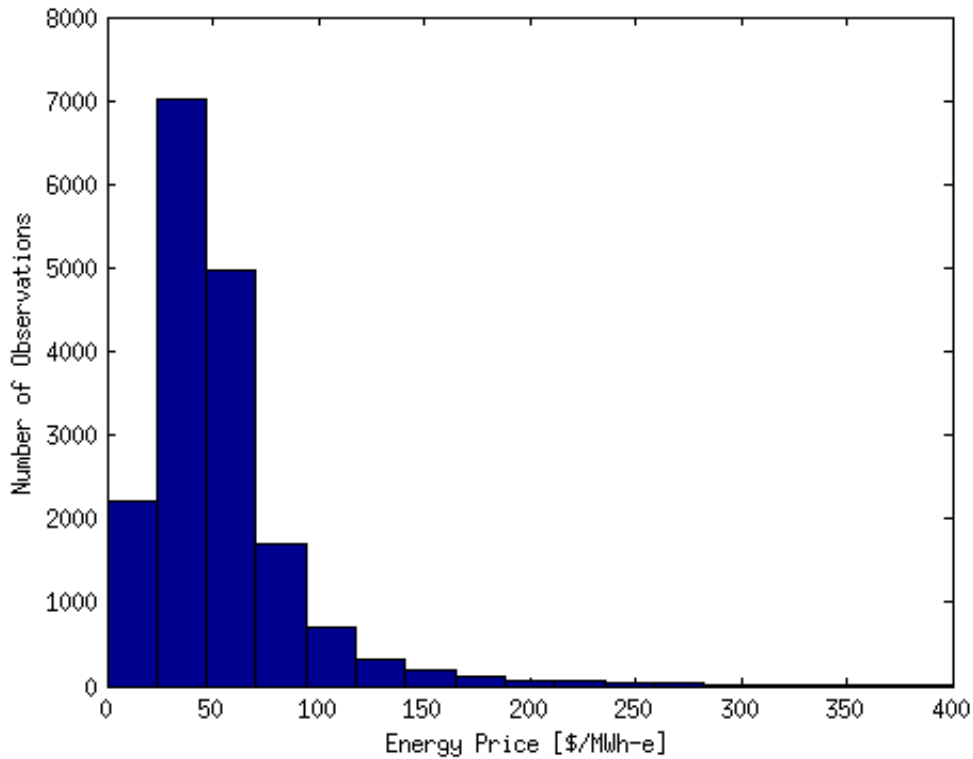
Figure 5. Histogram of wholesale energy prices over study period.[2]

As Denholm and Sioshansi [9, 10] note, a CSP plant consists of three interrelated components that can be sized differently. The first is the solar field, which is a field of mirrors that concentrates solar radiation onto a heat transfer fluid (HTF). The second is the powerblock, which is a heat engine that converts thermal energy into electricity. The third is the TES system, which can store thermal energy collected by the solar field for later use in the powerblock. The size of the powerblock is typically measured by its rated input or output capacities, which are measured in MW-t or MW-e, respectively. The size of the solar field can either be measured by the area that the mirrors cover or by using the concept of the solar multiple (SM). The SM scales the size of the solar field based on the size of the powerblock. A solar field with an SM of 1.0 is sized to provide sufficient thermal energy to operate the powerblock at its rated capacity with DNI of 950 W/m^2, a wind speed of 5 m/s, and an ambient temperature of 25° C. The size of the solar field scales relative to a field with an SM of 1.0 (e.g., a field with an SM of 1.7 is 70% larger than one with an SM of 1.0). The TES system has power and energy capacities. The power capacity, which is measured in MW-t, determines the maximum rate at which thermal energy can be charged or discharged from TES. We assume that the charging capacity of the TES system is scaled in proportion to the SM, so that the full output of the solar field can be stored if necessary. This is different from designs using indirect thermal energy storage, in which the heat exchanger used to transfer energy between the solar field heat transfer fluid and the thermal energy storage fluid is economically sized to only exchange energy that exceeds the thermal capacity of the powerblock. The energy capacity determines the maximum amount of energy that can be stored

---

[2] In addition there were 18 hours with prices negative prices and 24 hours with prices greater than $400/MWh.

7

in TES and is typically measured in MWh-t or by the number of hours of storage. We use the latter convention and define hours of storage as the number of hours that TES can be discharged at its maximum rated power capacity. TES systems in demonstration CSP plants have shown extremely high roundtrip efficiencies [5, 11-13].

CSP plants typically have solar fields that are oversized relative to the powerblock (i.e., SMs greater than 1.0). This is because a CSP plant with an SM of 1.0 will only allow the powerblock to operate at its nameplate capacity for a handful of hours during which DNI falling on the effective aperture of the solar field is at or near its annual maximum.[3] Increasing the SM will increase the capacity factor of the powerblock. However, if no TES is available, solar energy will be wasted during peak-solar hours since the solar field will collect more energy than the powerblock can feasibly use. This points to an added benefit of incorporating TES into a CSP plant, because it improves the economics of a larger field by increasing utilization of the powerblock.

Our optimization model consists of two parts. The first uses the Solar Advisor Model (SAM) [14]. SAM is a software package, based on the TRNSYS time-series simulation program [15], that simulates the dynamics of a CSP plant. SAM has been validated against empirical CSP operational data from the Solar Energy Generating Systems [16]. Weather data and CSP plant characteristics are input to SAM to determine how much thermal energy is collected by the solar field in each hour.[4]

The second part of our model is a mixed-integer program (MIP) that optimizes the operation of the CSP and wind plants to maximize revenues. This model takes hourly thermal energy collected by the solar field, as determined by SAM, potential generation from the wind plants, and energy prices as inputs. Wind data are obtained from the National Renewable Energy Laboratory's (NREL's) Western Wind Resource Dataset.[5] This dataset uses simulated hourly wind speed data to estimate the generation from a wind plant installed at a particular location. In order to account for the effects of geographic dispersion of wind plants, we use data for 56 locations around the study site, which can each accommodate up to 30 MW-e of wind. Price data are obtained from the ERCOT market operator and the ERCOT North zone price is used in the optimization, since we assume that the CSP and wind plant are connected by a radial transmission line going to this region [3]. The formulation of this MIP model is given in appendix A.

We assume that the CSP plants that we model have the same characteristics as the default parabolic trough system in SAM. This plant has a powerblock with a gross rated capacity of 110 MW-e, but can be run at 115% of this rated capacity. When the parasitic cooling and HTF pump loads are taken into the account, the maximum net capacity of the plant is about 120 MW-e. This plant includes a two-tank TES system, which we assume to have a roundtrip efficiency of 98.5% [9] and hourly heat losses of 0.031% of the energy in storage [4, 17]. We assume that the CSP plants have a SM of 2.0 and four hours of TES which is based on baseline plant designs in the

---

[3] The effective aperture considers cosine losses that occur due to non-normal incidence between the sun and the collectors
[4] Weather data used for this simulation are obtained from the National Solar Radiation Data Base, available for download at http://rredc.nrel.gov/solar/old data/nsrdb/.
[5] The Western Wind Resource Dataset is available for download at http://wind.nrel.gov/Web_nrel/.

CSP literature [8]. We also show selected results from cases where the plant has eight hours of TES.

We assume that the total nameplate capacity of the wind and CSP plants is 1,080 MW-e and consider cases in which there are between zero and nine CSP plants. Wind generators are then added to bring the nameplate capacity of the deployment to 1,080 MW-e. For instance, a deployment with four CSP plants would have a maximum CSP capacity of 480 MW-e and 600 MW-e of wind. We model cases in which the transmission lines connecting the deployment to the load center have a capacity of between 600 MW-e and 1,080 MW, meaning that we examine cases in which the transmission capacity of the deployment is as low as 56% of its generating capacity.

Although our analysis is based on a two-year period, we optimize the operation of the wind and CSP plants using a rolling 24-hour planning horizon. This process works by starting at the beginning of the study period and optimizing plant operations over a 48-hour period. The optimized dispatch for the first 24 hours is fixed and the algorithm rolls forward to the second day of the study period. We use the 48-hour optimization horizon to ensure that energy is kept in the TES system of the CSP plants if it would have carryover value on the following day [18]. Using a longer optimization horizon has little effect on revenues of a CSP plant [9]. Our optimization model further assumes that the generator has perfect foresight of weather and price data during each 48-hour optimization period. Relaxing this perfect foresight assumption has a limited effect on the profit and operation of a standalone CSP plant [9]. Because our analysis considers co-located wind and CSP that must share a limited transmission resource and wind generation patterns are less predictable than solar, it is likely that deployment profits are more sensitive to the perfect foresight assumption than would be for a standalone CSP plant.
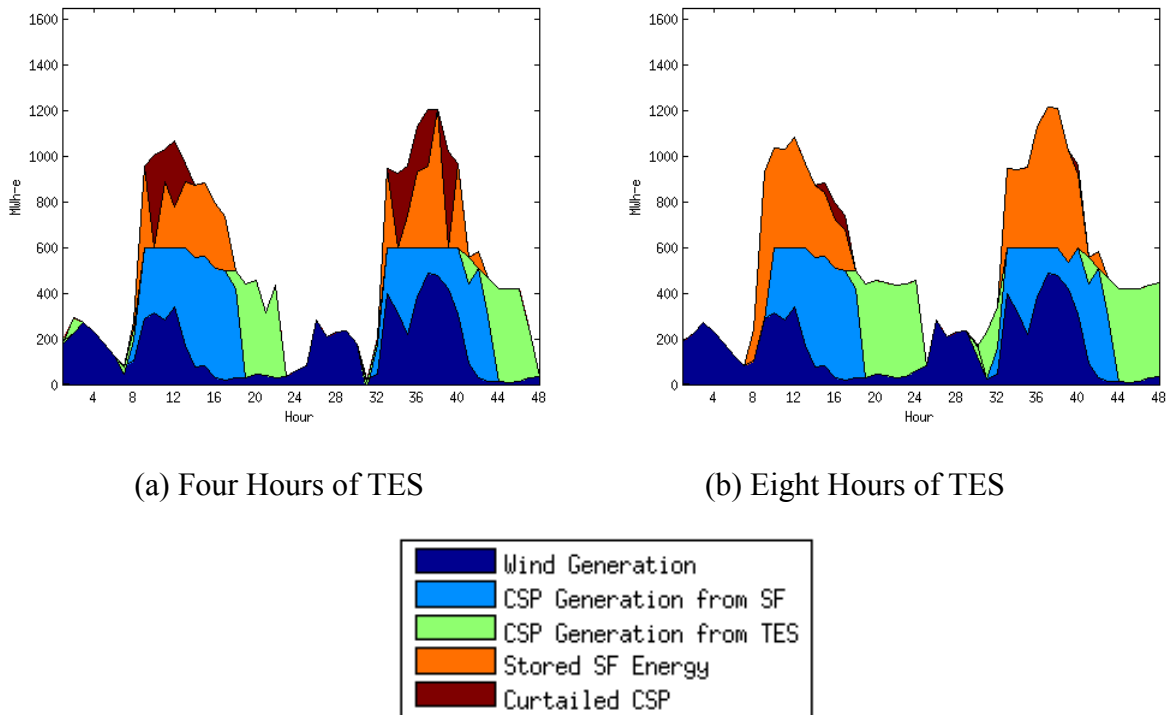
4　Results

4.1　Dispatch of Wind and CSP Deployments

Wind and CSP have two basic complementarities that potentially enable them to share transmission. One is that real-time wind and solar resource are often negatively correlated. The other is that CSP with TES is partially dispatchable, which allows solar generation to be shifted and to fill-in excess transmission capacity during subsequent hours with lower wind and solar resource. This allows for increased transmission utilization.

Figure 6 illustrates these complementarities by showing the dispatch of a deployment consisting of 480 MW-e of CSP with an SM of 2.0, 600 MW-e of wind, and 600 MW-e of transmission capacity over a two-day-long period beginning on May 16, 2004. Because the transmission line is sized at the maximum output of the wind plant, the maximum output of the combined wind and CSP system is 180% of the transmission capacity of the deployment. These days show some negative correlation between wind and solar resource—wind generation is relatively high overnight when there is zero solar resource and the solar peak lags the midday wind peak by at least two hours on both days. Thus, adding CSP allows for significantly greater transmission usage than if only wind is installed at this site. Figure 6 also demonstrates the other complementarity between wind and CSP, namely the ability of TES to store solar energy that would otherwise be curtailed. In the four-hour case roughly 32% of the energy collected by the solar fields is stored and used to produce energy later in the day when both solar and wind resources are near-zero and excess transmission capacity is available. Figure 6a also shows that despite this use of TES, about 21% of the thermal energy collected by the solar field is wasted due to the limited energy capacity of the system. The figure shows these curtailments in MWh-e by applying the average net efficiency (taking into account average parasitic loads) of the CSP plant. Despite this limitation, the four-hour TES system is able to reduce CSP curtailment by roughly 62% compared to a CSP plant without TES.[6] Adding eight hours of TES almost completely eliminates curtailment in this 48-hour period.

---

[6] Figure 6 shows that some of the thermal energy collected by the CSP plants is curtailed in hours 10 through 13, whereas there is no curtailment in hours 14 through 17 when all of the thermal energy is stored. This result is due to the fact that there are multiple optimal solutions of the dispatch model. For example more energy could be stored in hour 10 and energy in hour 14 curtailed while still satisfying the operating constraints of the TES system. Both solutions would yield the same profit-maximizing outcome. These multiple optima are also, in part, due to the perfect foresight assumption.

(a) Four Hours of TES   (b) Eight Hours of TES

Wind Generation
CSP Generation from SF
CSP Generation from TES
Stored SF Energy
Curtailed CSP

Figure 6. Example wind and CSP dispatch beginning May 16, 2004.

Note: Deployment includes 480 MW-e of CSP, 600 MW-e of wind, and 600 MW-e of transmission capacity. Figure 6a assumes CSP with four hours of TES, while Figure 6b assumes eight hours.

There are, however, limitations to these complementarities between CSP and wind. Some periods, which tend to occur in the spring, will have extended high wind generation, during which the TES system of the CSP plants will be filled and solar thermal energy will have to be curtailed due to the limited transmission. Figure 7 demonstrates this for the same deployment during a two-day period beginning on April 22, 2005. Figure 7a assumes the base case of four hours of TES and in this two-day period about 71% of the energy collected by the CSP plants' solar fields is curtailed. Overall, about 15% of the energy collected by the solar fields is curtailed annually, indicating that additional transmission or TES capacity may be desirable. Figure 7b shows the benefits of incorporating eight hours of TES, which somewhat reduces curtailment, and allows a more continuous output, for example largely filling the gap in hours 0 through 8 and 44 through 48. Figure 7a also shows that the model prioritizes wind over CSP. This is due both to the wind PTC, which makes wind $19/MWh-e more valuable than CSP from a marginal revenue perspective, and the higher variable operating and maintenance cost of CSP.[7]

---

[7]Our model only includes the $19/MWh-e Federal wind PTC. Other state and local incentives could provide wind with a further revenue advantage over CSP. Conversely, state and local PTCs for CSP could reduce the relative revenue advantage of wind. However, this prioritization will occur unless any such incentives are equal for the two technologies.
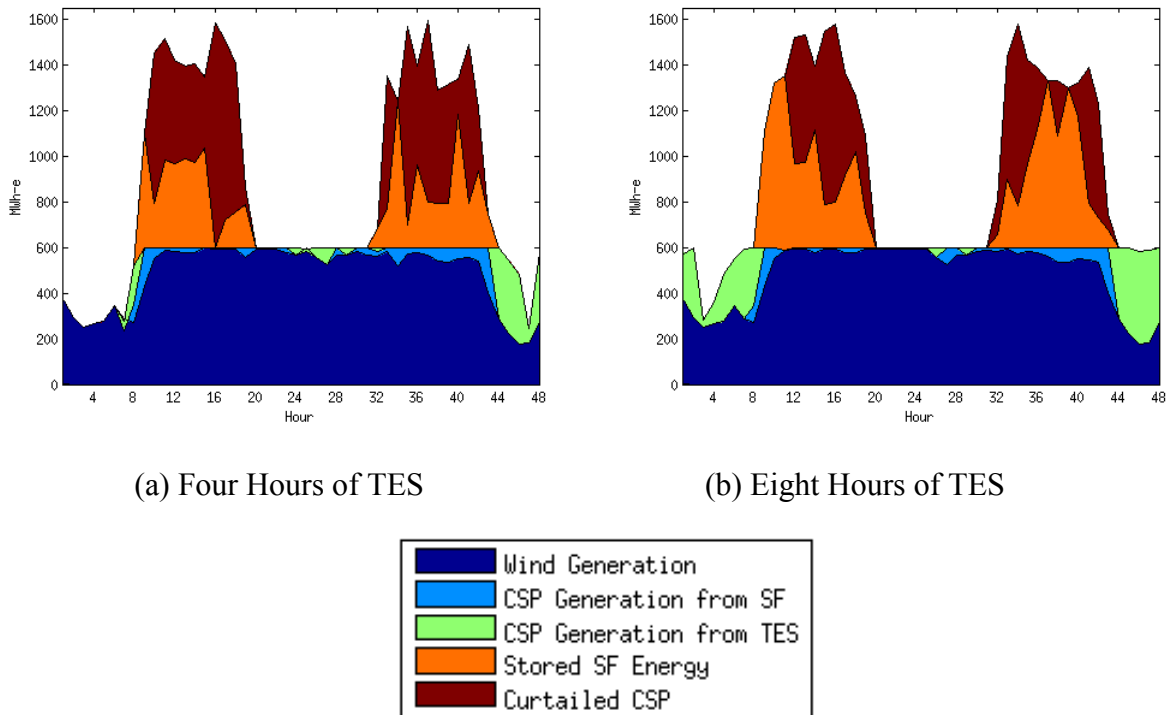
(a) Four Hours of TES   (b) Eight Hours of TES

Figure 7. Example wind and CSP dispatch beginning April 22, 2004.

Note: Deployment includes 480 MW-e of CSP, 600 MW-e of wind, and 600 MW-e of transmission capacity. Figure 7a assumes CSP with four hours of TES, while Figure 7b assumes eight hours.

Another limitation of having a downsized transmission link is that the CSP plant must be dispatched around wind generation and is operated in a suboptimal manner compared to a transmission-unconstrained deployment. This is illustrated in Figure 8, which shows the optimized dispatch of a deployment with 480 MW-e of CSP and 600 MW-e of wind during a three-day period beginning on October 17, 2004. For clarity, the dispatch of CSP is shown at the bottom of the figure. Figure 8a shows the operation of the deployment if there is no transmission constraint (i.e., there is 1,080 MW-e of transmission capacity). The figure shows that incorporating TES into the CSP plants allows the plant to sell energy during the highest-priced hours. For instance, stored thermal energy is discharged in hours 18, 30, and 62 when prices are relatively high.
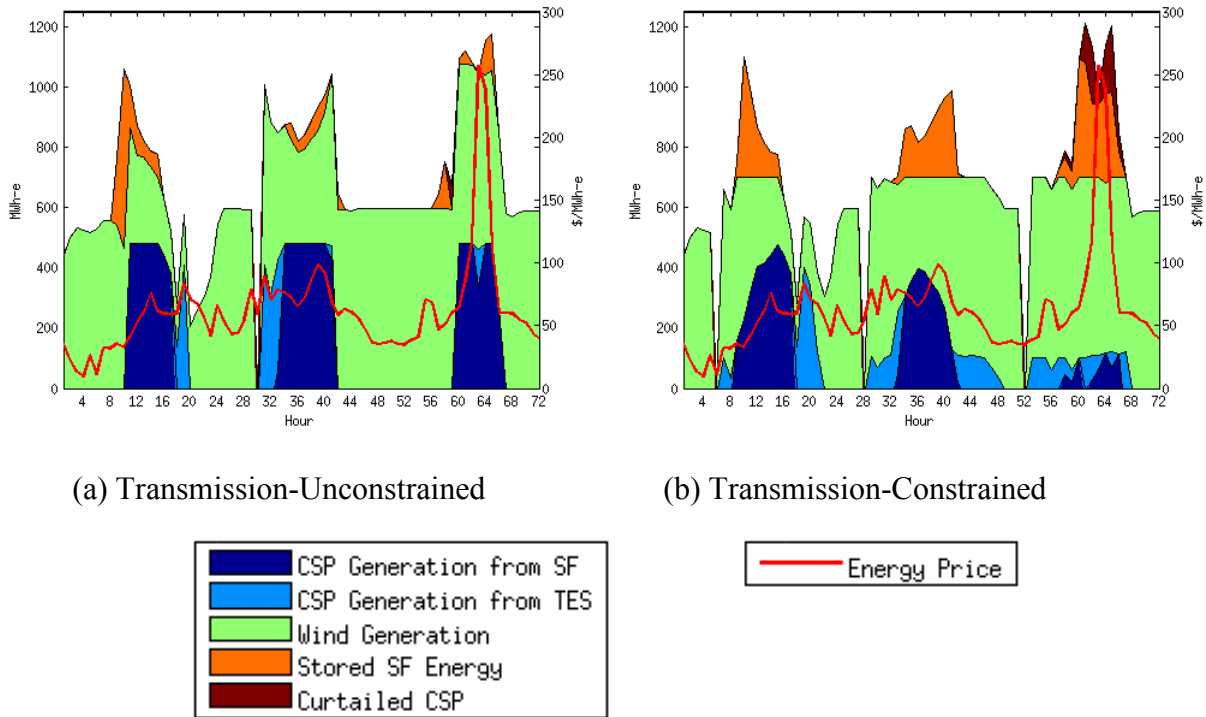
(a) Transmission-Unconstrained   (b) Transmission-Constrained

■ (dark blue)	CSP Generation from SF
■ (light blue)	CSP Generation from TES
■ (green)	Wind Generation
■ (orange)	Stored SF Energy
■ (dark red)	Curtailed CSP

—— (red line)	Energy Price

Figure 8. Example wind and CSP dispatch on October 17, 2004.

Note: Deployment includes 480 MW-e of CSP and 600 MW-e of wind capacity. Figure 8a is transmission-unconstrained and figure 8b has a 700 MW-e transmission capacity.

Figure 8b shows the operation of the same deployment on the same days with a 700 MW-e transmission line. The figure again demonstrates the benefit of TES in allowing CSP generation to be shifted to lower-resource hours. For instance, excess energy that would overload the transmission line in hours 9 through 15 is stored and discharged in hours 16 through 21 and 28 through 33, with similar behavior on the following days. However, this dispatch of the CSP plant is suboptimal from a market value standpoint. This is because the transmission constraint does not allow the CSP plant to sell as much energy during hours 30 through 33, when prices are relatively high. It must, instead, sell this energy in hours 42 through 49 when prices are lower. On the day shown in Figure 8, the average selling price of CSP energy is \$89.10/MWh-e in the transmission-unconstrained case, as opposed to only \$71.05/MWh-e with the constraint. Denholm and Sioshansi [3] demonstrate the same phenomenon when storage is co-located with a transmission-constrained wind generator. The operational policies shown in figure 8 and the resulting revenue differences represent a tradeoff between the cost and challenges of transmission development versus the optimal dispatch of CSP and TES.

4.2   Transmission Downsizing in Wind and CSP Deployments

Figures 6 and 7 point to the fundamental tradeoffs in deploying wind, CSP, and transmission. Reducing transmission capacity will increase the capacity factor of the transmission investment, but will also increase generator curtailment and decrease the value of the energy produced by the plant. Figures 8 through 12 explore these tradeoffs in greater depth. In addition to the base case with four hours of TES, the figures also include cases in which the CSP plants have eight hours

13

of TES. Figure 9 shows the capacity factor of the transmission line as a function of the transmission capacity and generation mix of the deployment. The transmission and CSP capacities are given as a percentage of the 1,080 MW-e generating capacity of the deployment. The wind generators that we model have capacity factors over the two years studied of about 33.9%, whereas the CSP plants with an SM of 2.0 and four hours of TES have a capacity factor of roughly 34.5%. Thus if the deployment is transmission-unconstrained, a CSP-only generation mix maximizes the capacity factor of the transmission link. For a smaller transmission link, however, it is beneficial to build a mix of wind and CSP, in order to exploit the negative correlation between wind and solar resource. The mix that maximizes transmission capacity factor ranges between 44% (480 MW-e) CSP with a 600 MW-e transmission link up to 89% (960 MW-e) CSP with 1,000 MW-e of transmission capacity.

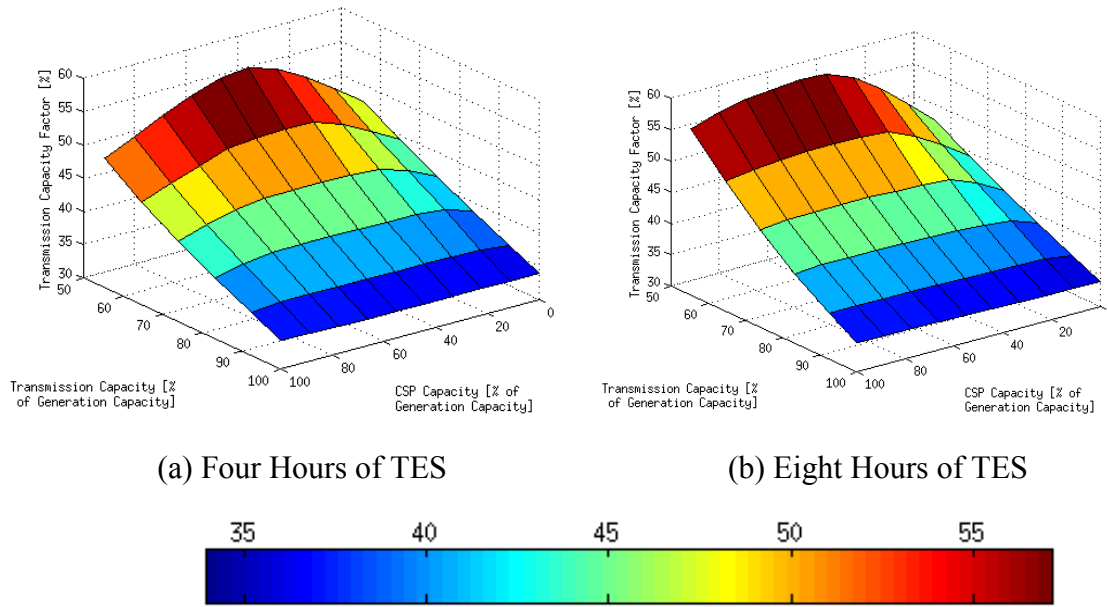(a) Four Hours of TES   (b) Eight Hours of TES

Figure 9. Capacity factor of the transmission line as a function of transmission capacity and generation capacity breakdown.

Note: Transmission and CSP capacities are given as a percentage of the 1,080 MW-e generating capacity of the deployment.

14

Figures 9 and 10 shows total energy curtailment as a function of the transmission capacity and generation mix of the deployment. Figure 10 shows total energy curtailments, while figure 11 shows CSP curtailments. Figure 11 shows that even in the transmission-unconstrained case there will be some CSP curtailment. This is because the solar field, which has an SM of 2.0, is oversized relative to the powerblock. Thus, in many hours, the solar field collects more thermal energy than can be used directly by the powerblock; while some of this energy can be stored, the energy capacity of the TES system limits the amount of such storage. Nevertheless, in the four-hour case, this curtailment is less than 2% of the 1,115 GWh-e of thermal energy collected by each CSP plant's solar field annually. For this reason, a wind-only deployment minimizes curtailment (since 100% of the potential wind generation is used) if the deployment is transmission-unconstrained. However, with a binding transmission constraint, a mix of wind and CSP minimizes curtailment. This is again because the negative correlation between real-time wind and solar availability yields a resource profile that results in fewer transmission constraint violations.

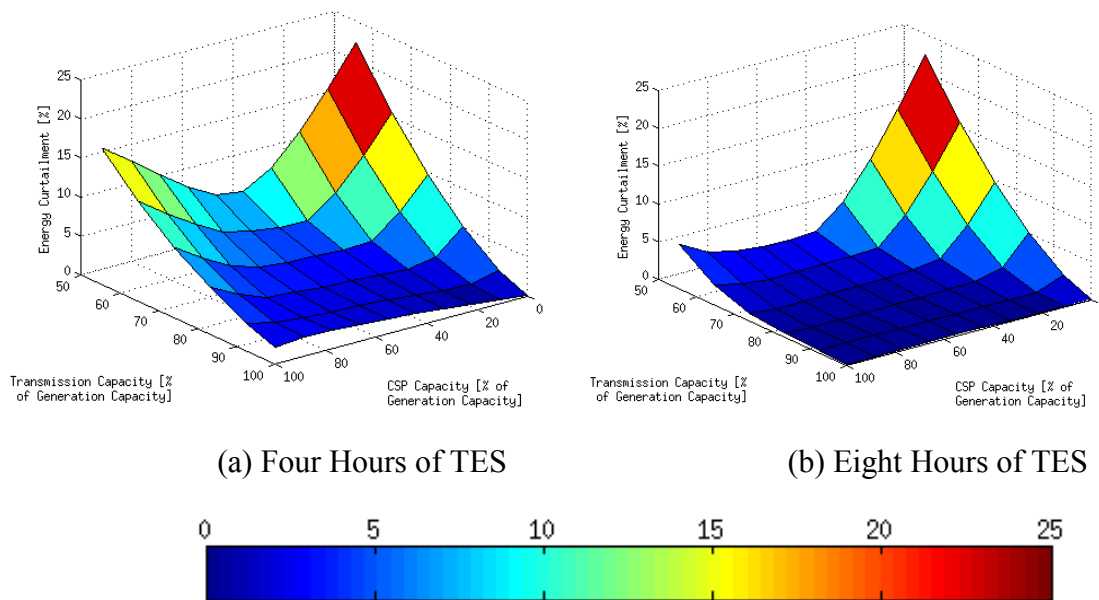(a) Four Hours of TES   (b) Eight Hours of TES

Figure 10. Total generation curtailed (both wind and CSP) as a function of transmission capacity and generation capacity breakdown.

Note: Transmission and CSP capacities are given as a percentage of the 1,080 MW-e generating capacity of the deployment.

15

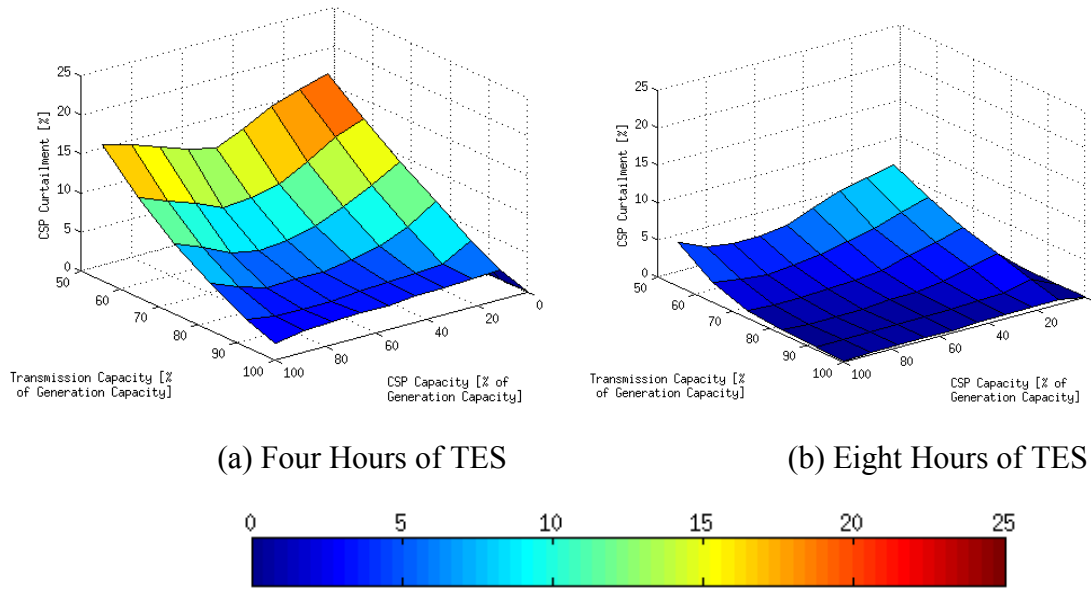(a) Four Hours of TES   (b) Eight Hours of TES

Figure 11. CSP Generation curtailed as a function of transmission capacity and generation capacity breakdown.

Note: Transmission and CSP capacities are given as a percentage of the 1,080 MW-e generating capacity of the deployment.

Figures 11 and 12 show the average selling price of energy from the deployment, excluding the wind PTC, as a function of the deployment configuration. Figure 12 shows the overall average selling price of wind and CSP generation, while figure 13 shows the average selling price of CSP generation only. Figure 12 shows that the overall average selling price of energy is increasing in the amount of CSP, which reflects two properties of CSP. One is that real-time solar availability tends to be highly correlated with system loads and prices. This correlation is because peak loads in the ERCOT system, which tend to be correlated with peak prices, are driven primarily by cooling needs, which is highly coincident with DNI. Wind, on the other hand, tends to be slightly negatively correlated with energy prices. This negative correlation is shown in Figure 12 since the average selling price of energy from a wind-only deployment is very slightly decreasing in the transmission capacity. As the transmission capacity of the deployment is decreased, wind generation is curtailed in high-wind hours, which tend to be low-price hours. The other property of CSP is its dispatchability. This dispatchability allows CSP generation to be shifted, within the constraints of the TES system and transmission link, to higher-priced hours. This generation shifting is advantageous because, while prices and solar resource tend to be correlated, they are not perfectly coincident. This is because cooling loads can often lag the peak in DNI by a few hours due to thermal inertia. Thus, adding TES to a CSP plant allows for further energy revenue increases.

16

(a) Four Hours of TES   (b) Eight Hours of TES

Figure 12. Average selling price of energy (both wind and CSP), excluding the wind PTC, as a function of transmission capacity and generation capacity breakdown.

Note: Transmission and CSP capacities are given as a percentage of the 1,080 MW-e generating capacity of the deployment.

(a) Four Hours of TES   (b) Eight Hours of TES
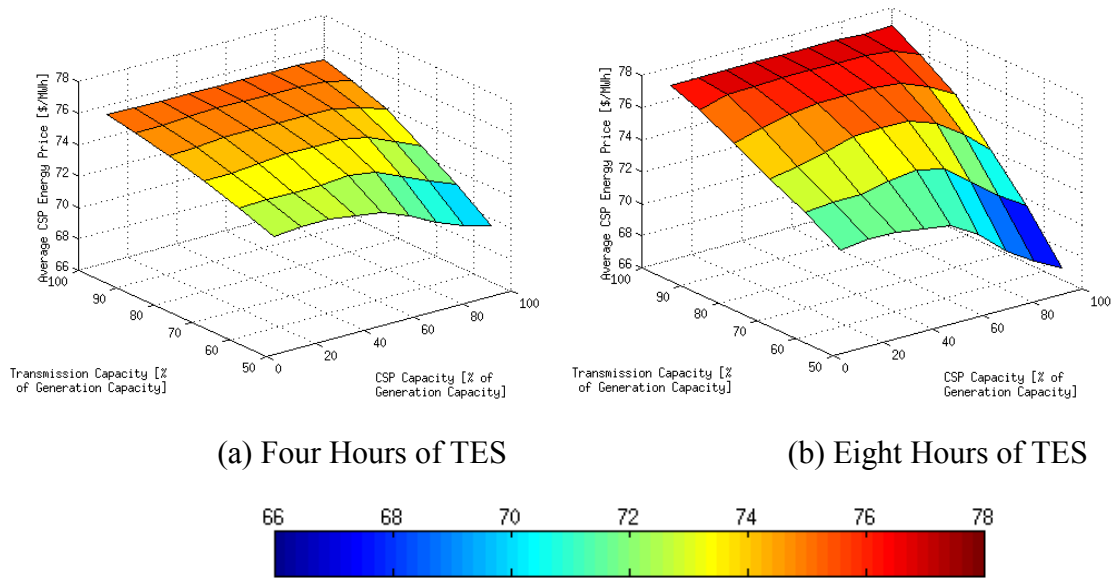
Figure 13. Average selling price of CSP generation as a function of transmission capacity and generation capacity breakdown.

Note: Transmission and CSP capacities are given as a percentage of the 1,080 MW-e generating capacity of the deployment.

17

Both Figures 11 and 12 show the effect of downsizing the transmission capacity, which is to diminish the value of TES. This is because CSP must share the scarce transmission with wind, as illustrated by the example in Figure 6. Thus, as the transmission capacity of the deployment is reduced, TES is decreasingly used to shift solar energy to high-price hours and is used instead to shift stored energy to low-wind and low-solar hours. Figure 13 also shows that increasing the amount of CSP in a deployment reduces the average selling price of CSP. This is, again, because the limited transmission capacity forces TES to be increasingly used to shift CSP generation to lower-price hours. As transmission constraints increase, the reduction in average price in the eight-hour TES case is due to the fact that while additional TES allows more energy to be sold, it tends to dispatch in lower-price hours. This means that the benefits of reduced curtailment associated with larger amounts of TES are somewhat offset by the lower value of this additional energy.

Figures 13 and 14 illustrate how this interaction between transmission and TES impacts deployment revenues. The figure shows average annual revenues as a function of the deployment configuration. Figure 14 shows total energy revenues from wind and CSP, excluding the wind PTC, and Figure 15 shows CSP energy revenues only. The figure shows that CSP earns considerably higher energy revenues than wind. This is both due to CSP having a slightly higher capacity factor (i.e., producing more energy) and because CSP produces higher-value energy due to the coincidence between DNI and prices and the use of TES. The figure also shows that downsizing transmission can significantly reduce deployment revenues. This has a greater effect on CSP—in the four-hour TES case, reducing the transmission capacity from 1,080 MW-e to 600 MW-e reduces annual CSP revenues by 26% (which amounts to $61 million for an all-CSP deployment), whereas it reduces wind revenues by 22% (which is $36 million for an all-wind deployment). The greater effect on CSP reflects the fact that much of the added value of CSP derives from its ability to use TES to deliver energy during high-price hours, which is limited when the transmission constraint is imposed. Figure 14 also shows the small total revenue difference between 4 and 8 hours of storage in CSP-only systems without transmission constraints.

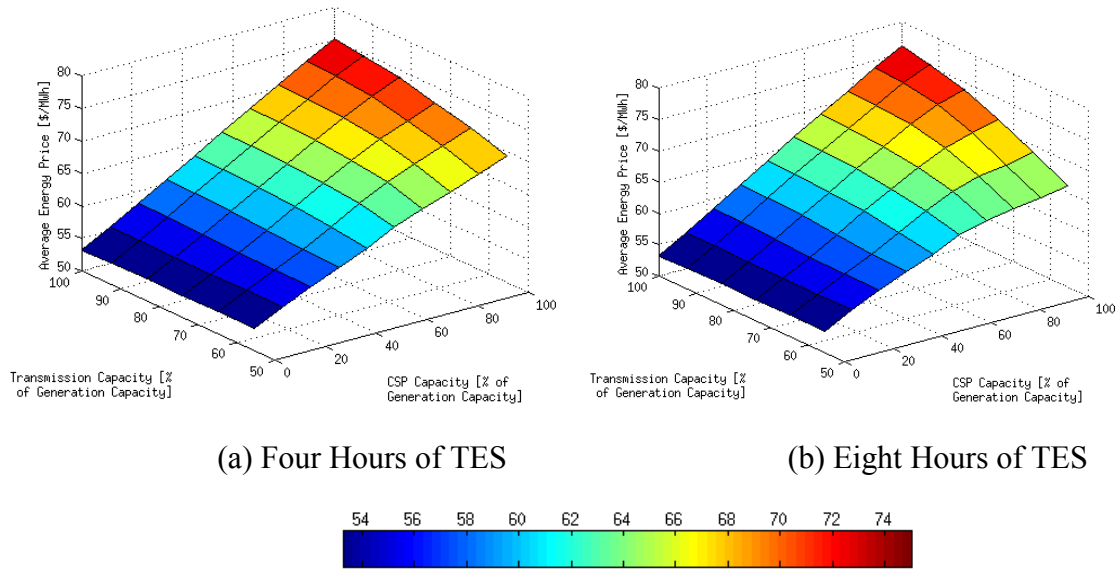(a) Four Hours of TES   (b) Eight Hours of TES
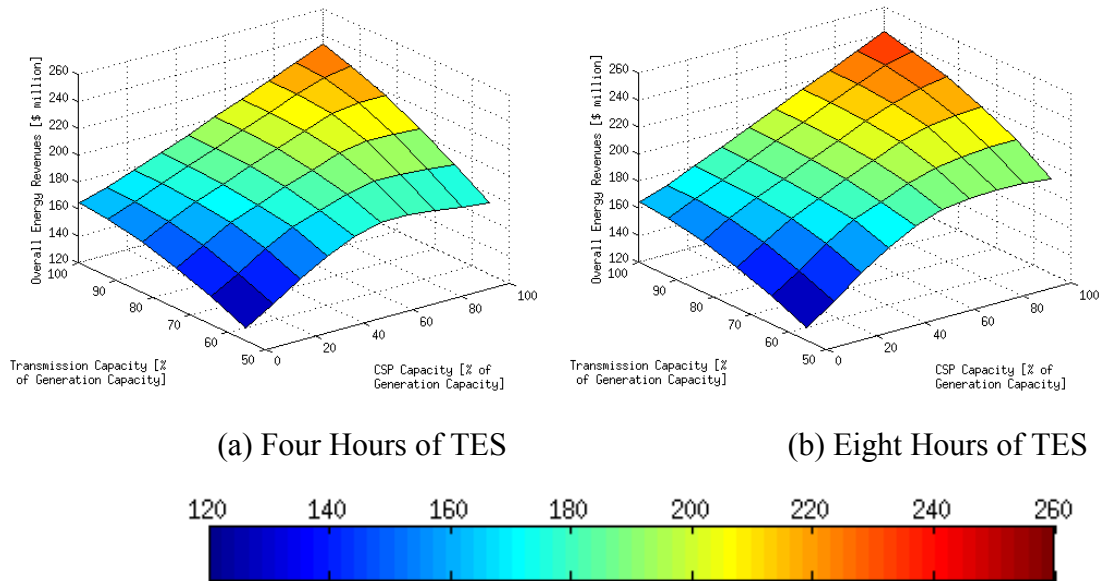
Figure 14. Average annual energy revenues (both wind and CSP), excluding the wind PTC, as a function of transmission capacity and generation capacity breakdown.

Note: Transmission and CSP capacities are given as a percentage of the 1,080 MW-e generating capacity of the deployment.

(a) Four Hours of TES   (b) Eight Hours of TES

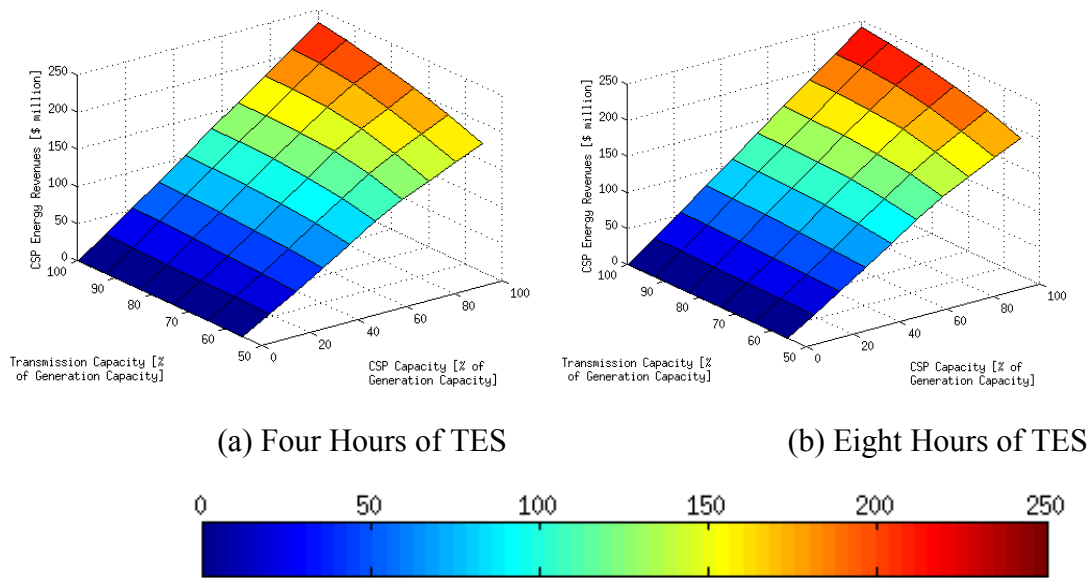**Figure 15. Average CSP annual energy revenues, as a function of transmission capacity and generation capacity breakdown.**

Note: Transmission and CSP capacities are given as a percentage of the 1080 MW-e generating capacity of the deployment.

19

4.3 Long-Term Economics of Co-Located Wind and CSP Deployments

The analysis done thus far assumes the configuration of a deployment and analyzes short-term operational decisions. A related question is what deployment configuration would maximize long-term economic value. Such an analysis would require comparing upfront capital costs against discounted revenue streams over the lifetime of the different deployments. This type of an analysis presents four challenges. One is that we only have two years of time-coincident wind and solar resource data, which limits our ability to estimate revenues over the full lifetime of a deployment. A second is that the cost of utility-scale CSP is rather uncertain due to fluctuations in commodity prices and the potential for substantial manufacturing improvements. A third is that the cost competitiveness of wind and CSP relative to conventional generating technologies will depend on future policy decisions, such as carbon regulation and fuel prices and subsidies. Finally, this analysis does not consider the impact of the increased use of renewables on the ERCOT market, mix of generators and the value of dispatchable resources, such as CSP with TES.

In light of these and other factors that can affect long-term investment decisions, we opt to use revenue estimates over the two years modeled to derive breakeven costs for the different deployments. The breakeven cost in this analysis is defined as the highest capital cost for the deployment that will make an investment economic on the basis of the revenue stream that we estimate. We also combine our revenue estimates with wind, CSP, and transmission cost forecasts to estimate a year-1 return on investment (ROI), which is the fraction of the investment cost of different deployments that is recovered through annual revenues. This analysis focuses on the more conservative case with only four hours of TES in the CSP plants. We first discuss the revenue, cost, and subsidy assumptions used in our analysis.

4.3.1 Revenue Estimates

We assume that the wind and CSP deployments receive two revenue streams—energy and capacity payments. Energy revenues are estimated based on the optimized value of the objective function used in the optimization model. Capacity payments are supplemental payments made to a generator for the capacity that it provides the system. Generators that are added to a system increase system reliability by reducing the probability that there will be insufficient generating capacity in real-time to meet system loads. Capacity payments are intended to monetize this benefit. The capacity payment of a deployment is given by the price of system capacity times the capacity value of the deployment. We assume that the price of capacity is based on the capital cost of a natural gas-fired combustion turbine, which is estimated at $625/kW-e in 2005 dollars [19]. We use the cost of a combustion turbine since this is a generation technology that is often used for peak-capacity purposes.

We use the operational performance of the deployments to estimate their capacity value. A number of different capacity value estimation techniques have been applied to wind [20-36] and CSP [37]. These include reliability theory-based methods and capacity factor-based approximations. One of the challenges raised in estimating the capacity value of CSP plants with TES is that one must account for both how much energy the generator plans to produce in each hour and how much energy is in the TES system. This is because even though the CSP generator may plan to produce relatively little energy, the thermal energy in the TES system could be used in real-time to help avert a system capacity shortage. This could happen, for example, if energy

prices during an hour are relatively low and it is optimal (from an energy revenue-maximization perspective) to keep energy stored as opposed to generate.

One proposed method that accounts for this capability of TES is to use the optimized dispatch of the CSP plant, as determined by the optimization model, to determine the maximum amount of energy that could be produced in each hour using the energy stored in TES [37, 38]. This maximum potential generation in each hour is then used to estimate the capacity value using a capacity factor-based approximation. We use such a technique, the details of which are given in appendix B.

Figure 16 shows the capacity value of the deployments as a function of the deployment configuration. The capacity values are given as a percentage of the 1,080 MW-e nameplate generating capacity of the deployments. The figure shows that CSP plants tend to have higher capacity values than wind generators, which is consistent with previous findings [20-37]. This is both because of the coincidence between solar resource availability and peak loads, as well as the dispatchability of CSP with TES. Since TES is used to shift solar energy to the highest-price hours, and because energy prices are strongly correlated with system loads and the likelihood of a system outage, optimizing TES to maximize energy revenues will also tend to increase the capacity value of CSP.
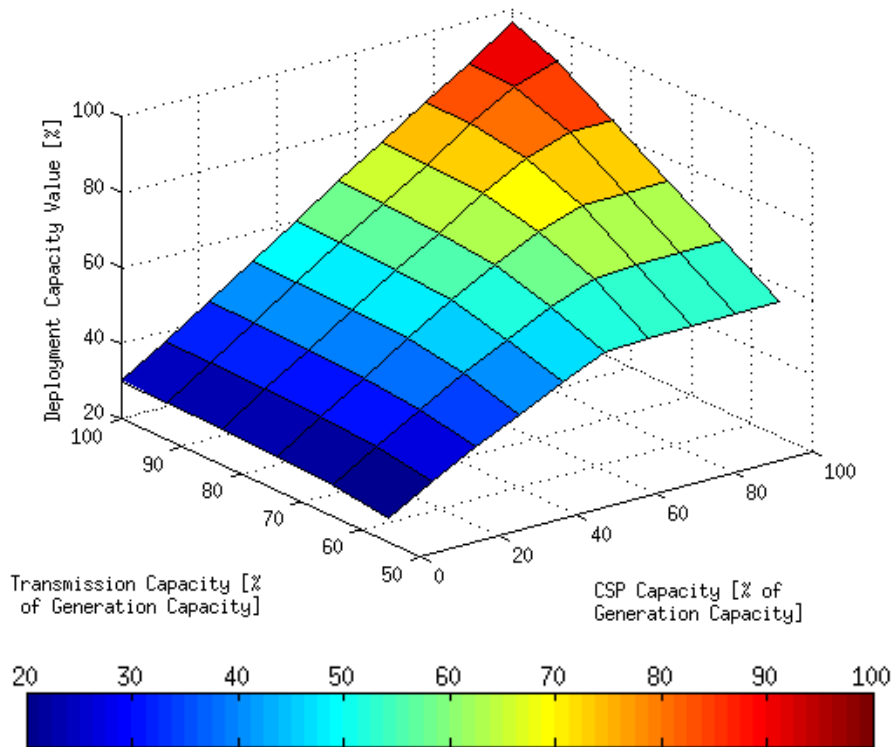

Figure 16. Capacity value of deployments as a function of transmission capacity and generation capacity breakdown.

Note: Capacity value and transmission and CSP capacities are given as a percentage of the 1,080 MW-e generating capacity of the deployment.

21

4.3.2 Cost Estimates

Our ROI calculations take into consideration capital costs associated with wind, CSP, and transmission construction, as well as CSP variable generation costs. A recent estimate places the capital cost of wind at about $1,650/kW in 2006 dollars [19]. We deflate this to $1,598/kW in 2005 dollars using consumer price index (CPI) data provided by the U.S. Department of Labor's Bureau of Labor Statistics.[8] CSP is assumed to have a variable cost of $0.70/MWh-e, which is included in the optimization model and in our cost calculations. Turchi *et al*. [8] provide forecasts of 2020 CSP construction costs in 2010 dollars. We break these costs into three components—a solar field cost that is proportional to the SM of a plant, a TES cost that is proportional to hours of storage in the TES system, and a fixed balance of plant cost, which includes the powerblock. The TES costs assume that the charging capacity of the TES system is equal to the nameplate power capacity of the powerblock, and do not account for the larger charging capacity that we assume. If this larger charging capacity is used in the default trough system modeled in SAM, the cost of TES increases by about 20% relative to the smaller charging capacity. Thus we inflate the TES costs reported by Turchi *et al*. [8] by this amount to arrive at the cost of the TES system that we model. Because of fluctuations in component costs, we deflate the costs reported in 2010 dollars to 2005 dollars using the Chemical Engineering Plant Cost Indices.[9] Table 2 summarizes the costs used in our analysis.

Table 2. Per-Plant CSP Construction Costs in 2005 Dollars

Component	Cost
Fixed ($ million)	129.69
Solar Field ($ million/SM)	133.00
TES ($ million/hour)	10.59

Figure 17 shows historical transmission construction cost data from a variety of ac and high-voltage dc (HVDC) projects built between 1995 and 2008 [3]. The data shown are for projects rated at 500 MW-e or greater and the costs are adjusted to 2005 dollars using CPI data. The figure shows that the costs vary significantly among the projects, and could possibly reflect site-specific differences. Nevertheless, most projects have costs between $200/km-MW-e and $800/km-MW-e, and we use these as potential bounding values on the cost of transmission for our deployments. The length of the transmission line is assumed to be 12% greater than the linear distance between the deployment and the interconnection point, based on the characteristics of the Intermountain Power Project from Utah to southern California [39].

---

[8]These data are available at http://www.bls.gov/data/inflation_calculator.htm.
[9]These indices are available at http://www.che.com/pci/.
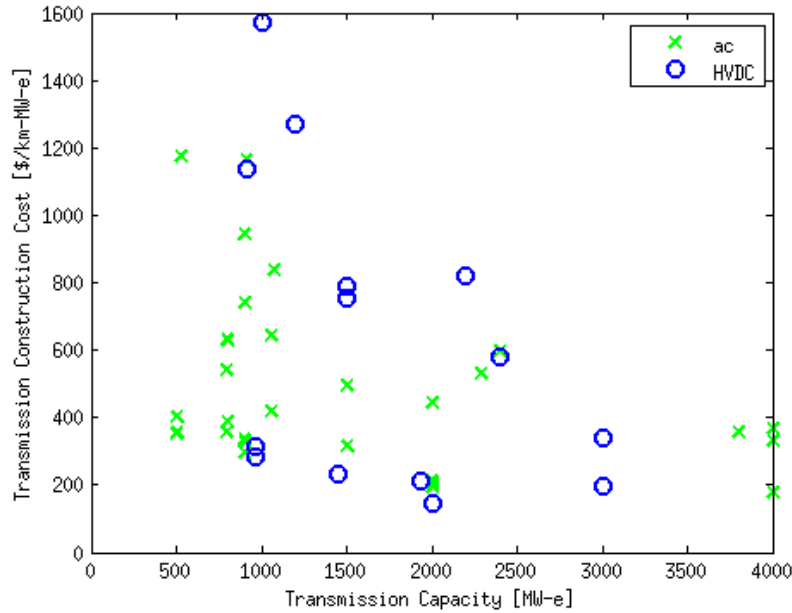
Figure 17. Historical transmission construction costs

4.3.3 Deployment Subsidies

Wind and solar generators are currently offered a variety of subsidies under Federal, state, and local law. Our analysis focuses on Federal subsidies. These include a $19/MWh-e PTC for wind (based on its value in our analysis year of 2005), and a 30% investment tax credit (ITC) on the upfront capital cost of solar. We assume that this ITC applies only to the CSP plants themselves, and excludes supplemental costs such as transmission. We include both of these subsidies in computing ROIs but exclude them in deriving breakeven costs. We exclude them from breakeven cost calculations because doing so would require an assumption about the capital cost of CSP relative to wind and transmission (in order to determine what fraction of the cost to apply the ITC to).

4.3.4 Deployment Breakeven Costs

In order to compare the annual revenues of the deployments that we estimate to a long-term capital investment, we use a capital charge rate (CCR). The CCR captures all of the financing parameters and translates the total cost of the investment (including principal and financing) into an annual cost [3]. We assume an 11% CCR. The breakeven cost is defined as the net annual profit of the deployment from energy and capacity payments, less variable CSP generation costs, divided by the CCR. We can express the breakeven cost of a deployment as:

$$\frac{\varphi^e + \varphi^c - \varphi^v}{\psi^{CCR}},$$

where φ^e and φ^c denote annual energy and capacity revenues, respectively, of the deployment, φ^v denotes the associated annual variable cost of CSP generation, and ψ^{CCR} denotes the CCR.

23

Figure 18 shows breakeven costs for different deployment configurations. The breakeven costs are divided by the 1,080 MW-e nameplate generating capacity of the deployments to give a $/MW-e value. As shown previously, CSP plants tend to earn significantly higher revenues than wind generators. Thus when the deployment is transmission-unconstrained, a CSP-only deployment yields the highest breakeven cost. As the transmission capacity is reduced, however, a mix of wind and CSP maximizes revenues and the breakeven cost. This is because shifting the generation mix toward wind reduces solar generation that would be curtailed due to the transmission constraint, while increasing deployment generation overnight when wind resources are higher. Thus the breakeven cost-maximizing deployment configuration ranges between 78% (840 MW-e) CSP with 600 MW-e of transmission capacity and 67% (720 MW-e) CSP with 800 MW-e of transmission.
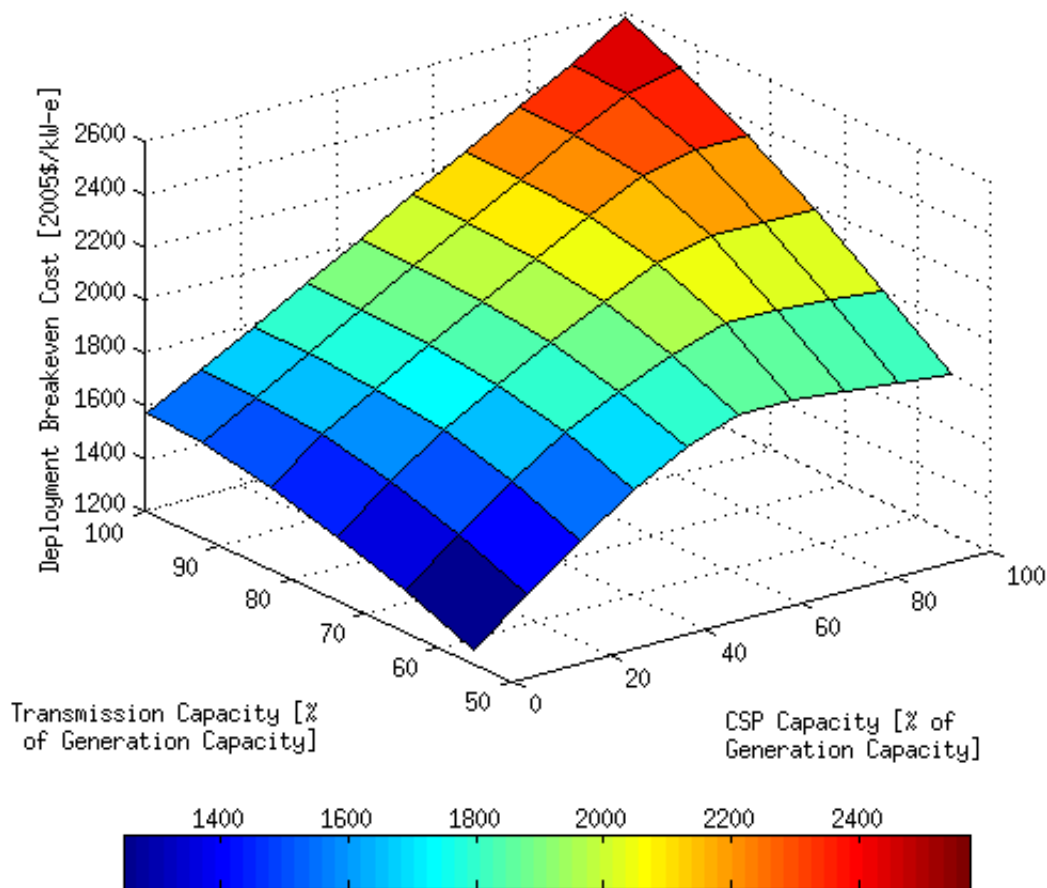

Figure 18. Deployment breakeven cost as a function of transmission capacity and generation capacity breakdown.

Note: Breakeven cost and transmission and CSP capacities are given as a percentage of the 1,080 MW-e generating capacity of the deployment. CSP plants are assumed to have an SM of 2.0 and four hours of TES.

4.3.5 Deployment Investment Cost Recovery

Our ROI calculations compare the annual revenues that a deployment earns from energy and capacity sales and the wind PTC to the total capital cost of the deployment. Deployments with an ROI that is at least as great as the CCR are said to be economic, since the annual revenues earned are greater than the annualized cost of the investment. If we define φ^p as the wind PTC earned by a deployment and χ^w, χ^s, and χ^t as the capital cost of the wind, CSP, and transmission components of the deployment, and ψ^{ITC} as the solar ITC rate, then the ROI of the deployment is given by:

$$\frac{\phi^e + \phi^c + \phi^p - \phi^v}{\chi^w + (1 - \psi^{ITC}) \cdot \chi^s + \chi^t}.$$

Figure 19 shows the ROI of deployments, as a function of their transmission capacity and generation capacity breakdown. Figure 19a assumes a transmission cost of \$200/km-MW-e, while figure 19b uses a cost of \$800/km-MW-e. Deployments that have an ROI of at least 11% (which is our assumed CCR) are denoted with magenta circles and the deployment with the highest ROI is denoted with a black cross.

(a)   (b)
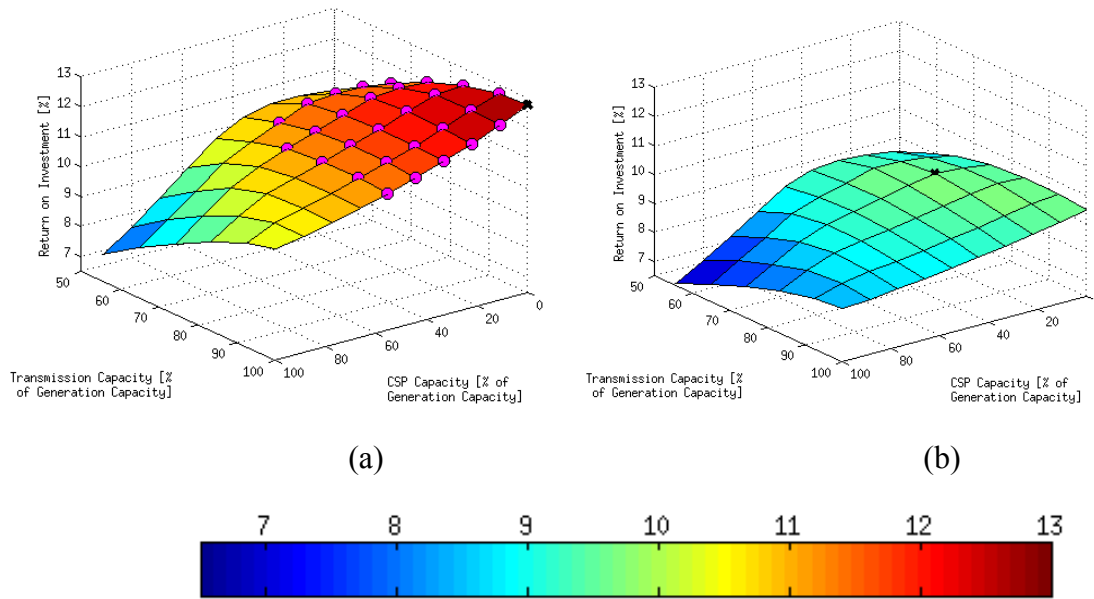
Figure 19: Deployment ROI as a function of transmission capacity and generation capacity breakdown.

Note: Transmission and CSP capacities are given as a percentage of the 1,080 MW-e generating capacity of the deployment. Deployments with an ROI of at least 11% are denoted by a magenta circle. Deployments that maximize ROI are denoted by a black cross. Figure 19a assumes a transmission cost of \$200/km-MW-e and figure 19b assumes a transmission cost of \$800/km-MW-e.

25

Comparing figures 18a and 18b shows deployment economics are highly sensitive to the cost of transmission. There are no economic deployments if the cost of transmission is greater than about \$485/km-MW-e. However there are a number of deployment configurations with transmission capacities as low as 700 MW-e and up to 56% CSP on a capacity and energy basis that are economic. Figure 19b shows that the ROI-maximizing deployment with the higher transmission cost has a transmission link that is downsized relative to its generating capacity. Moreover, when four hours of TES is incorporated into the CSP plants, a deployment with 22% CSP, on a capacity and energy basis, is ROI-maximizing, yielding an ROI of about 9.7%.

It should be noted that these results represent a snapshot of deployments in historic market conditions. Escalation in costs of conventional generation, restrictions on carbon emissions, and other factors could increase the value of the systems studied here. Furthermore, while some of the value of dispatchable CSP is captured by the assumed capacity payment, additional values of dispatchable energy, such as the provision of ancillary services could add further revenues [9]. Finally the value of dispatchable energy could change as a function of increased penetration of variable wind (and solar PV), and this could also change the likely configuration of CSP plants, including differing amounts of TES.

5 Conclusions

This report discusses and analyzes the potential benefits of co-locating wind and solar generation in the southwestern United States. Such a deployment strategy can improve the capacity factor of the combined plant and the associated transmission investment, with dispatchable CSP shifting energy to periods during reduced wind output. However, adding transmission constraints associated with co-location reduces performance, including the inability of CSP to provide maximum output during periods of both high demand and significant wind output. Furthermore, even with the use of TES, there are periods of extended high wind output and high solar output, which can result in curtailed energy. Despite these limitations, we do find cases in which a mix of CSP and wind can be justified by market revenues, and that in some cases deployments with up to 56% CSP capacity yield a positive net ROI. This will depend on a substantial reduction in CSP costs. Deployment economics are highly sensitive to transmission development costs, which have varied significantly in past projects, as well as future prices of conventional energy and potential restrictions on carbon emissions.

Appendix A. MIP Model Formulation

To give the formulation of the MIP model, we first define the following problem parameters and sets:

T	set of hours in optimization horizon,
C	set of CSP plants,
κ	transmission capacity (MW-e),
λ	transmission losses,
p_c^s	charging capacity of TES system of CSP plant c (MW-t),
p_c^d	discharge capacity of TES system of CSP plant c (MW-t),
h_c	hours of charging capacity of TES system of CSP plant c,
η_c	hourly heat losses of TES system of CSP plant c,
ρ_c	roundtrip efficiency losses of CSP plant c,
e_c^-	minimum power capacity of powerblock of CSP plant c (MW-t),
e_c^+	maximum power capacity of powerblock of CSP plant c (MW-t),
$f_c(\cdot)$	heat rate function of powerblock of CSP plant c,
$g_c^{HTF}(\cdot)$	HTF pump parasitics function of CSP plant c,
$g_c^{BOP}(\cdot)$	balance of plant parasitics function of CSP plant c,
e_c^{SU}	startup energy requirement of powerblock of CSP plant c (MWh-t),
α_c	variable cost of CSP plant c ($/MWh-e),
π_t	price of energy in hour t ($/MWh-e),
$e_{c,t}^{SF}$	thermal energy collected by solar field of CSP plant c in hour t,
$\overline{w}_t$	total wind energy available in hour t, and
γ	wind production tax credit ($/MWh-e).

We also define the following decision variables:

$l_{c,t}$ storage level of TES of CSP plant c at the end of hour t,

$s_{c,t}$ energy storage by TES of CSP plant c in hour t,

$d_{c,t}$ energy discharged from TES of CSP plant c in hour t,

$\sigma_{c,t}$ binary variable that equals 1 if TES of CSP plant c is being charged in hour t,

$e_{c,t}^{PB}$ energy put into powerblock of CSP plant c in hour t,

$e_{c,t}^{net}$ net generation from CSP plant c in hour t,

$u_{c,t}$ binary variable that equals 1 if powerblock of CSP plant c is online in hour t,

$r_{c,t}$ binary variable that equals 1 if powerblock of CSP plant c is started up in hour t,

w_t wind generated in hour t,

n_t^s gross electricity energy sold in hour t,

n_t^p gross electricity energy purchased in hour t, and

n_t binary variable that equals 1 if energy is being sold in hour t.

The formulation of the model is then given by:

$$\text{m} \quad \sum_{t \in T} \left(a\pi_t \cdot (n_t^s - n_t^p) + \gamma \cdot w_t - \sum_{c \in C} \alpha_c e_{c,t}^n \right) \tag{1}$$

$$\text{s.t.} \quad \frac{n_t^s}{1-\lambda} - (1-\lambda)n_t^p = w_t + \sum_{c \in C} e_{c,t}^n, {}^\epsilon \qquad \forall\, t \in T; \tag{2}$$

$$-\kappa \leq \frac{n_t^s}{1-\lambda} - (1-\lambda)n_t^p \leq \kappa, \qquad \forall\, t \in T; \tag{3}$$

$$0 \leq n_t^s \leq \kappa \cdot n_t, \qquad\qquad\qquad \forall\, t \in T; \tag{4}$$

$$0 \leq n_t^p \leq \kappa \cdot (1 - n_t) \qquad\qquad \forall\, t \in T; \tag{5}$$

$$l_{c,t} = \eta_c \cdot l_{c,t-1} + s_{c,t} - d_{c,t}, \qquad \forall\, c \in C\; t \in T; \tag{6}$$

$$0 \leq l_{c,t} \leq h_c \cdot p_c^s, \qquad\qquad\quad \forall\, c \in C\; t \in T; \tag{7}$$

$$0 \leq s_{c,t} \leq \sigma_{c,t} \cdot \text{m} \quad e_{c,t}^{S}\}, {}^{F}p_c^s\} \qquad \forall\, c \in C\; t \in T; \tag{8}$$

$$0 \le d_{c,t} \le (1 - \sigma_{c,t}) \cdot p_c^d, \qquad\qquad \forall\, c \in C\ t, \in T; \qquad (9)$$

$$1 - u_{c,t} \le \sigma_{c,t}, \qquad\qquad \forall\, c \in C\ t, \in T; \qquad (10)$$

$$s_{c,t} - \rho_c \cdot d_{c,t} + e_{c,t}^P + {}^B e_c^S \cdot {}^U r_{c,t} \le e_{c,t}^S, \qquad\qquad \forall\, c \in C\ t, \in T; \qquad (11)$$

$$e_{c,t}^n \stackrel{e}{=} f_c^t(e_{c,t}^P) - {}^B g_c^H\ (d_{c,t}^T) - {}^F g_c^B\ (e_{c,t}^{QP}) \qquad\qquad \forall\, c \in C\ t, \in T; \qquad (12)$$

$$e_c^- \cdot (u_{c,t} - r_{c,t}) \le e_{c,t}^P \le {}^B e_{c,t}^+ \cdot (u_{c,t} - r_{c,t}) \qquad\qquad \forall\, c \in C\ t, \in T; \qquad (13)$$

$$u_{c,t} - u_{c,t-1} \le r_{c,t}, \qquad\qquad \forall\, c \in C\ t, \in T; \qquad (14)$$

$$\sigma_{c,t}, u_{c,t}, r_{c,t}, n_{c,t} \in \{0,1\} \qquad\qquad \forall\, c \in C\ t, \in T;\ \text{and} \qquad (15)$$

$$0 \le w_t \le \overline{w}_t,\ . \qquad\qquad \forall\, c \in C\ t, \in T. \qquad (16)$$

Objective function (1) maximizes revenues from net energy sales and the wind production tax credit (PTC), net of CSP generation costs. We assume a variable operations and maintenance cost of \$0.70/MWh-e. Constraint set (2) defines gross energy sales and purchases in terms of wind and CSP generation by ensuring that all net energy generated is bought or sold.

Constraint set (3) imposes the transmission limit on net sales (the sum of wind and CSP generation must be less than or equal to the transmission capacity). Constraint sets (4) and (5) force the generator to only sell or purchase energy at a given time. Constraint set (6) defines the amount of energy in each CSP plant's TES as a function of the previous storage level, plus any net energy charged into TES. Constraint set (7) limits the amount of energy in storage to be within the size of the TES reservoir. Constraint sets (8) and (9) impose power limits on TES charging and discharging. They also prevent the TES system from charging and discharging energy simultaneously. Constraint set (10) forces the CSP plant to discharge TES only when the powerblock is online. A CSP plant without TES can be modeled using this same framework, by setting p_c^s, p_c^d, and h_c equal to zero.

Constraint set (11) limits the net amount of thermal energy used by each CSP plant to be no more than the amount of energy collected by its solar field. Constraint set (12) defines net generation of the CSP plants based on the heat rate function and the parasitic loads of the HTF pumps and balance of plant. The HTF pumps must be operated whenever TES is discharged, while the balance of plant parasitics account for cooling tower and other component loads. Constraint set (13) imposes the upper and lower bounds when the powerblock is online. It also assumes that the powerblock takes an hour to startup, during which time it does not produce energy. Constraint set (14) defines powerblock startups in terms of transitions in the 'online' state variables. Constraint set (15) imposes integrality constraints on the state variables. Constraint set (16) restricts wind generation to be less than available wind.

Appendix B. Capacity Factor Estimation Technique

We estimate the capacity factor of the deployments based on the optimized operation of each deployment given by maximizing objective function (1) subject to constraints (2) through (16). This optimized dispatch is used to compute the maximum amount of energy that the deployment could produce in each hour. To define this maximum generation we first define the maximum potential thermal energy that can be delivered to the powerblock of each CSP plant in each hour as:

$$\widetilde{e}_{c,t}^{P} = \min\left\{\overline{B}\,0, \min\left\{e_{c}^{+}, e_{c,t}^{S} + \rho_{c}^{F}, \min\left\{\overline{p}_{c}^{d}, \eta_{c}\{l_{c,t-1}\}\right\}\right\} - e_{c}^{S}\right\} \cdot (1 - u_{c,t}^{U})\right\}. \tag{17}$$

Equation (17) defines the maximum thermal energy as the minimum of the rated capacity of the powerblock and the sum of energy collected by the solar field and energy in TES (with associated energy losses taken into account). Equation (17) further assumes that the powerblock can be started up immediately (using the required thermal energy) in the event of a system shortage event. We next define the amount of this energy that is taken from TES as:

$$\widetilde{d}_{c,t} = \widetilde{e}_{c,t}^{P,B} - e_{c,t}^{S,F}.$$

The maximum potential outputs of the CSP plants are then given by:

$$\widetilde{e}_{c,t}^{n} = f_{c}^{t}(\widetilde{e}_{c,t}^{P})^{B} g_{c}^{H} (\widetilde{d}_{c,t}^{T})^{F} g_{c}^{B} (\widetilde{e}_{c,t}^{P}).$$

We finally compute the maximum amount of energy that the deployment can provide as:

$$\widetilde{n}_{t}^{s} = (1 - \lambda) \cdot \min\left\{\kappa, \overline{w}_{t} + \sum_{c \in C} \widetilde{e}_{c,t}^{n}\right\}.$$

We use the quantities, $\widetilde{n}_{t}^{s}$, to estimate the capacity value of the deployment using a capacity factor-based approximation. A number of different capacity factor-based approximations have been applied to wind and CSP. These methods approximate the capacity value of the plant as its average capacity factor during the hours with the highest loads or loss of load probabilities (LOLPs). A third method uses the average capacity factor during the hours with the highest LOLPs, but also weights the capacity factor in each hour by the corresponding system LOLP. Studies show that the LOLP-weighted method provides the most robust capacity value estimates [21, 37]. In the case of wind, using the 10% of the hours of the year with the highest LOLPs provides the most robust capacity value estimate, whereas using the top-10 hours provides the most robust estimate for a CSP plant. Because our analysis considers a mix of wind and CSP plants, we opt to use the top-10% LOLP hours of the year, since the capacity value estimate of a CSP plant is less sensitive to this parameter.

To estimate the capacity value of the deployment we first define the weight used in each hour as:

$$\omega_t = \frac{\zeta_t}{\sum_{\tau \in \hat{T}} \zeta_\tau},$$

where $\hat{T}$ is the set of hours used in the approximation and ζ_t is the LOLP in hour t. In our case, $\hat{T}$ denotes the 10% of the hours in each year that have the highest LOLPs. The capacity value estimate is then given by:

$$v = \sum_{t \in \hat{T}} \omega_t \cdot \tilde{n}_t^s.$$

We compute the LOLPs of the system using load data from the ERCOT system operator and generator data from Form 860 data collected by the U.S. Department of Energy's Energy Information Administration. These data specify the nameplate capacity and generating technology of each conventional plant in the ERCOT system. These are combined with historical effective forced outage rate data from the North American Electric Reliability Corporation's Generating Availability Data System.

References

1. Lower Colorado River Authority. "Study of Electric Transmission in Conjunction with Energy Storage Technology." Prepared for Texas State Energy Conservation Office, Austin, TX. August 2003.

2. Wiser, R.; Bolinger, M. *2010 Wind Technologies Market Report*. 98 pp.; NREL, Tech. Rep. NREL/TP-5000-51783; DOE/GO-102011-3322. June, 2011.

3. Denholm, P; Sioshansi, R. "The value of compressed air energy storage with wind in transmission-constrained electric power systems," *Energy Policy*, vol 37, pp 3149-3158, 2009.

4. Pacheco, J. E. Gilbert, R. *Overview of recent results of the solar two test and evaluations program*. Sandia National Laboratories, Tech. Rep. SAND99-0091C, 1999.

5. Herrmann, U.; Kearney, D. W. "Survey of thermal energy storage for parabolic trough power plants." *Journal of Solar Energy Engineering*, vol 124, pp 145-152, 2002.

6. Price, H.; Lüpfert, E.; Kearney, D.; Zarza, E.; Cohen, G.; Gee, R.; Mahoney, R. "Advances in parabolic trough solar power technology," *Journal of Solar Energy Engineering*, vol 124, pp 109-125, 2002.

7. *Assessment of parabolic trough and power tower solar technology cost and performance forecasts*. NREL, Tech. Rep. NREL/SR-550-34440, 2003.

8. Turchi, C.; Mehos, M.; Ho, K.; Kolb, G. J. *Current and Future Costs for Parabolic Trough and Power Tower Systems in the US Market*. NREL, Tech. Rep. NREL/CP-5500-49303, 2010.

9. Sioshansi, R.; Denholm, P. *The value of concentrating solar power and thermal energy storage*." NREL, Tech. Rep. NREL/TP-6A2-45833, 2010.

10. Sioshansi, R.; Denholm, P. "The value of concentrating solar power and thermal energy storage," *IEEE Transactions on Sustainable Energy*, vol 1, pp 173-183, 2010.

11. Kearney, D. W.; Kelly, B.; Herrmann, U.; Cable, R.; Pacheco, J. E.; Mahoney, A. R.; Price, H.; Blake, D. M.; Nava, P.; Potrovitza, N. "Engineering aspects of a molten salt heat transfer fluid in a trough solar field," *Energy*, vol 29, pp 861-870, 2004.

12. Gil, A.; Medrano, M.; Martorell, I.; Lázaro, A.; Dolado, P.; Zalba, B.; Cabeza, L. F. "State of the art on high temperature thermal energy storage for power generation. part 1—concepts, materials and modellization." *Renewable and Sustainable Energy Reviews*, vol 14, pp 31-55, 2010.

13. Pacheco, J. E.; Showalter, S. K.; Kolb, W. J. "Development of a molten-salt thermocline thermal storage system for parabolic trough plants." *Journal of Solar Energy Engineering*, vol 124, pp 153-159, 2002.

14. Gilman, P.; Blair, N.; Mehos, M.; Christensen, C.; Janzou, S. *Solar advisor model user guide for version 2.0*. NREL, Tech. Rep. NREL/TP-670-43704, 2008.

15. Fiksel, A.; Thornton, J. W.; Klein, S. A.; Beckman, W. A. "Developments to the TRNSYS simulation program," *Journal of Solar Energy Engineering*, vol 117, pp 123-127, 1995.

16. Price, H. *Parabolic trough solar power plant simulation model*. NREL, Tech. Rep. NREL/CP-550-33209, 2003.

17. Herrmann, U.; Kelly, B.; Price, H. "Two-tank molten salt storage for parabolic trough solar power plants," *Energy*, vol 29, pp 883-893, 2004.

18. Sioshansi, R.; Denholm, P.; Jenkin, T.; Weiss, J. "Estimating the Value of Electricity Storage in PJM: Arbitrage and Some Welfare Effects." *Energy Economics*, vol 31, pp 269-277, 2009.

19. *20% Wind Energy by 2030. Increasing Wind Energy's Contribution to U.S. Electricity Supply*. DOE/GO-102008-2567. July, 2008.

20. Milligan, M. R. *Measuring wind plant capacity value*. NREL, Tech. Rep. NREL/TP-441-20493, 1996.

21. Milligan, M. R.; Parsons, B. "Comparison and case study of capacity credit algorithms for wind power plants." *Wind Engineering*, vol 23, pp 159-166, 1999.

22. Milligan, M. R.; Factor, T. "Optimizing the geographic distribution of wind plants in Iowa for maximum economic benefit and reliability." *Wind Engineering*, vol 24, pp 271-290, 2000.

23. Milligan, M. R.; Porter, K. "The capacity value of wind in the United States: Methods and implementation." *The Electricity Journal*, vol 19, pp 91-99, 2006.

24. Pudaruth, G. R.; Li, F. "Capacity credit evaluation: A literature review." Presented at the Third International Conference on Electric Utility Deregulation and Restructuring and Power Technologies, pp 2719-2724, 2008.

25. Milligan, M. R.; Parsons, B. *Comparison and case study of capacity credit algorithms for intermittent generators*. NREL, Tech. Rep. NREL/CP-440-22591, 1997.

26. D'Annunzio, C.; Santoso, S. "Noniterative method to approximate the effective load carrying capability of a wind plant." *IEEE Transactions on Energy Conversion*, vol 23, pp 544-550, 2008.

27. Milligan, M. R.; Porter, K. *Determining the capacity value of wind: An updated survey of methods and implementation*. NREL, Tech. Rep. NREL/CP-500-43433, 2008.

28. Söder, L.; Amelin, M. "A review of different methodologies used for calculation of wind power capacity credit." Presented at 2008 IEEE Power and Energy Society General Meeting, 2008.

29. Ensslin, C.; Milligan, M.; Holttinen, H.; O'Malley, M.; Keane, A. "Current methods to calculate capacity credit of wind power, IEA collaboration." Presented in the 2008 IEEE Power and Energy Society General Meeting. 2008.

30. Amelin, M. "Comparison of capacity credit calculation methods for conventional power plants and wind power." *IEEE Transactions on Power Systems*, vol 24, pp 685-691, 2009.

31. Haslett, J.; Diesendorf, M. "The capacity credit of wind power: A theoretical analysis." *Solar Energy*, vol 26, pp 391-401, 1981.

32. Söder, L.; Bubenko, J. "Capacity credit and energy value of wind power in hydro-thermal power system." Published in proceedings of the 9th Power Systems Computation Conference. 1987.

33. Bernow, S.; Biewald, B.; Hall, J.; Singh, D. *Modelling renewable electric resources: A case study of wind.* Oak Ridge National Laboratory, Tech. Rep. ORNL/Sub-93-03370, 1994.

34. El-Sayed, M. A. H. "Substitution potential of wind energy in Egypt." *Energy Policy*, vol 30, pp 681-687, 2002.

35. Kahn, E. P. "Effective load carrying capability of wind generation: Initial results with public data." *The Electricity Journal*, vol 17, pp 85-95, 2004.

36. Milligan, M. R. *Modeling utility-scale wind power plants part 2: Capacity credit.* NREL, Tech. Rep. NREL/TP-500-29701, 2002.

37. Madaeni, S. H.; Sioshansi, R., Denholm, P. *Capacity Value of Concentrating Solar Power Plants.* NREL, Tech. Rep. NREL/TP-6A20-51253, 2011.

38. Tuohy, A.; O'Malley, M. "Impact of pumped storage on power systems with increasing wind penetration." Published in proceeding of the Power & Energy Society General Meeting, pp 1-8, 2009.

39. Wu, C. T.; Shockley, P. R.; Engstron, L. "The Intermountain Power Project 1600 MW HVDC Transmission System." *IEEE Transactions on Power Delivery*, vol 3, pp 1249-1256, 1988.